Stable triaxiality at the highest spins in ^{138}Nd and ^{139}Nd

C. M. Petrache,[1] G. Lo Bianco,[2] D. Ward,[3] A. Galindo-Uribarri,[4] P. Spolaore,[5] D. Bazzacco,[1] T. Kröll,[1] S. Lunardi,[1]
R. Menegazzo,[1] C. Rossi Alvarez,[1] A. O. Macchiavelli,[3] M. Cromaz,[3] P. Fallon,[3] G. J. Lane,[3] W. Gast,[6] R. M. Lieder,[6]
G. Falconi,[2] A. V. Afanasjev,[7,8] and I. Ragnarsson[9]

[1]*Dipartimento di Fisica and INFN, Sezione di Padova, Padova, Italy*
[2]*Dipartimento di Matematica e Fisica, University of Camerino, Camerino, Italy*
[3]*Nuclear Science Division, Lawrence Berkeley National Laboratory, Berkeley, California 94720*
[4]*Physics Division, Oak Ridge National Laboratory, Oak Ridge, Tennessee 37831*
[5]*INFN, Laboratori Nazionali di Legnaro, Legnaro, Italy*
[6]*Institut für Kernphysik, Forschungszentrum Jülich, D-52425 Jülich, Germany*
[7]*Physik-Department, Technische Universität München, D-85747 Garching, Germany*
[8]*Laboratory of Radiation Physics, Institute of Solid State Physics, University of Latvia, LV 2169, Salaspils, Latvia*
[9]*Department of Mathematical Physics, Lund Institute of Technology, Lund, Sweden*
(Received 6 October 1999; published 17 December 1999)

The nuclei ^{138}Nd and ^{139}Nd have been studied at very high spins via the ^{48}Ca$+^{94}$Zr reaction. Several new rotational bands were observed, four in ^{138}Nd and two in ^{139}Nd. The $J^{(2)}$ moments of inertia calculated from the observed γ-ray energies are very small and almost constant, indicating that these bands are triaxial. Cranked Nilsson-Strutinsky calculations reproduce the general behavior of the bands, supporting this interpretation and suggesting an approximately constant γ value of $\sim+35°$ over a large spin range up to the highest observed spins. These bands and a few similar bands in other nuclei of the $N\approx80$ region are a unique example of almost undisturbed triaxial bands.

PACS number(s): 21.60.Ev, 21.10.Re, 27.60.+j

The large-deformation bands observed to date in the light Nd nuclei are based on configurations which are stabilized by the $Z=60$ and $N=72,74$ shell gaps, developing in the Nilsson diagram at a quadrupole deformation of $\varepsilon_2\approx0.3$ [1–3]. The general properties of these bands, including the measured quadrupole moments [4], clearly support the interpretation that at high spins they correspond to a second minimum of the potential energy surfaces with $\varepsilon_2\approx0.3-0.35$ (the first minimum, corresponding to the ground state band, has a smaller deformation with $\varepsilon_2\approx0.15-0.25$). Going towards $N=82$ one expects a smooth variation in the deformation of the second minimum from prolate ($\gamma\sim0°$) to triaxial ($\gamma\sim+30°$), as predicted by cranked Nilsson-Strutinsky (CNS) calculations with either Woods-Saxon [1] or Nilsson [3] potentials.

Bands interpreted as triaxial have been observed at high spin in the $A=130-140$ mass region for ^{136}Nd [5], ^{133}Ce [6], and ^{134}Ce [7]. The general features of these bands have been well reproduced in calculations with $\gamma\sim-30°$, i.e., triaxial shapes with rotation along the intermediate axis. However, none of these bands show any specific experimental fingerprint which can be associated with triaxial deformation.

In Eu isotopes with neutron numbers $N=79,80,81$, several bands with irregular behavior were observed at high spins and were interpreted as triaxial with $\gamma\sim+30°$ [8]. These bands have an unusually low $J^{(2)}$ moment of inertia outside the band crossing regions indicating small collectivity, typical of triaxial shapes with $\gamma>0°$. The small moments of inertia were, however, not reproduced by the paired calculations presented in Ref. [8]. Furthermore, two bands showing similar features have been observed in ^{137}Nd, but no explicit interpretation has been given [9].

In order to investigate the shape evolution of intruder configurations when approaching the $N=82$ shell closure, an experiment has been performed to search for high-spin collective bands in the ^{138,139}Nd nuclei. Several new high-spin bands were identified. They have small $J^{(2)}$ moments of inertia which can be related to a low collectivity. Such behavior is reproduced in the unpaired calculations presented below. The corresponding configurations show a stable triaxial deformation ($\gamma\approx+35°$) which stays essentially constant over the full spin range where the bands are observed.

The ^{48}Ca$+^{94}$Zr reaction has been used with a 195 MeV ^{48}Ca beam of 2–3 pnA provided by the 88-Inch Cyclotron at the Lawrence Berkeley National Laboratory. Two self-supporting ^{94}Zr foils of 380 μg/cm^2 enriched to 98% were used as the target. Gamma-ray coincidences were measured with the 8π spectrometer which comprises 20 HPGe detectors with bismuth germanate (BGO) anti-Compton shields and an inner ball of 71 BGO scintillator detectors. Events were written to tape when at least two HPGe detectors (after suppression) and 10 BGO detectors of the inner ball fired in coincidence.

The chosen reaction mainly populates the ^{138}Nd and ^{139}Nd nuclei through the evaporation of four and three neutrons, respectively. E_γ-E_γ coincidence matrices were constructed with proper conditions on the sum γ-ray energy (H) and multiplicity (K) registered in the BGO ball, selected to enhance long rotational cascades in the nuclei of interest. The matrix used in the data analysis contained 0.58×10^9 events with multiplicity $K>22$ and a suitable lower cut on H, which enhance the 3n and 4n channels at the expense of the 5n and 6n channels. The multipolarity of the transitions was deduced from a directional correlation from oriented states (DCO) analysis as described in Ref. [10].
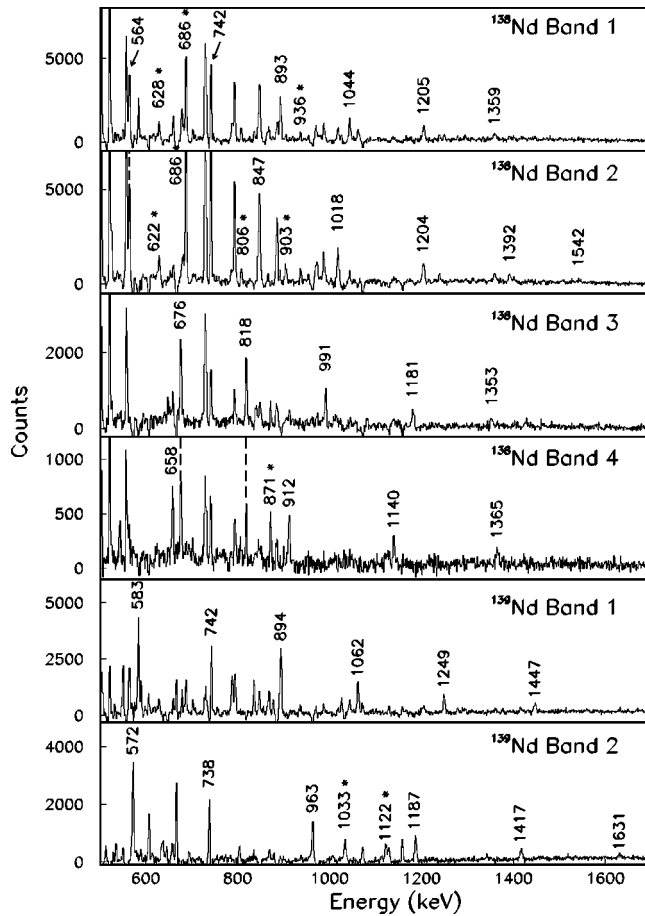
FIG. 1. Sum coincidence γ-ray spectra obtained by gating on the transitions within the six observed bands in ^{138}Nd and ^{139}Nd. The gates were set only on the in-band transitions indicated by their energies in each panel. The out-of-band transitions are marked by an asterisk.

High-spin states in ^{138}Nd have been previously studied by Müller-Veggian *et al.* [11] and de Angelis *et al.* [12] up to spin 19 and 21, respectively, whereas the level scheme of ^{139}Nd has been studied by Gizon *et al.* [13] and Müller-Veggian *et al.* [11] up to spin 29/2. The present experiment confirms the main features of the previously proposed level schemes. A complete discussion of our results, which led to the construction of very rich level structures at moderate and high spins, will be presented in a separate paper. The present work reports only the collective bands populated at the highest spins.

Four new bands in ^{138}Nd and two new bands in ^{139}Nd have been found. Coincidence γ-ray spectra for each band are shown in Fig. 1. The assignment of the bands to a specific nucleus was made on the basis of clear coincidence relationships with γ-ray transitions already known in the two nuclei. The decay out of band 1 of ^{138}Nd towards the low-lying levels is fragmented (see Fig. 2), probably due to the mixing of the lowest levels with the highest states of the previously observed $(\pi h_{11/2})^2$ band [12], and was therefore only partially observed. Among the various possible deexcitation pathways, the most clear one is through a 936 keV transition of $E2$ character, which links the second level of
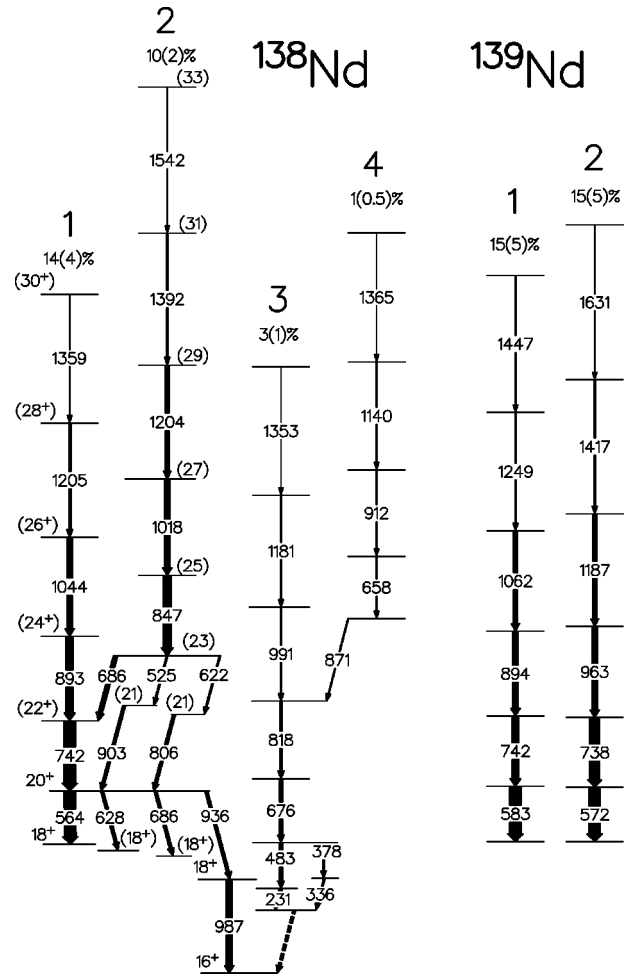

FIG. 2. Partial level schemes for ^{138}Nd and ^{139}Nd showing the triaxial bands and their decay-out paths. The intensity relative to the total population of each nucleus is written on top of each band. The lowest 16^+ and 18^+ states in ^{138}Nd were known from previous investigations [12].

band 1 to the 18^+ state of the $(\pi h_{11/2})^2$ band. We therefore assign spin-parity 20^+ to the second level of band 1. The lowest level assigned to band 1 is the one populated by the intense 564 keV $E2$ transition and has spin 18^+. The states populated by the 564, 628 and 686 keV transitions also have a fragmented decay, which could not be firmly established from the present data.

Band 2 of ^{138}Nd feeds into the lowest states of band 1. Its lowest observed state decays by means of a 686 keV $\Delta I = 1$ γ ray into the 22^+ state of band 1 and by means of two cascades consisting of the $622(E2)$-$806(\Delta I = 1)$ and $525(E2)$-$903(\Delta I = 1)$ keV γ rays into the 20^+ level of the same band. We therefore assign spin 23 to the lowest observed state of band 2.

The decay out of band 3 could not be established in any detail. From the feeding pattern of the known low-lying states it is likely that the state populated by the 483 keV transition at the bottom of band 3 has spin 18. Band 4 decays to band 3 by means of the 871 keV transition, which has a stretched-dipole character according to its measured DCO ratio. With the previous spin assignment for band 3, the spin
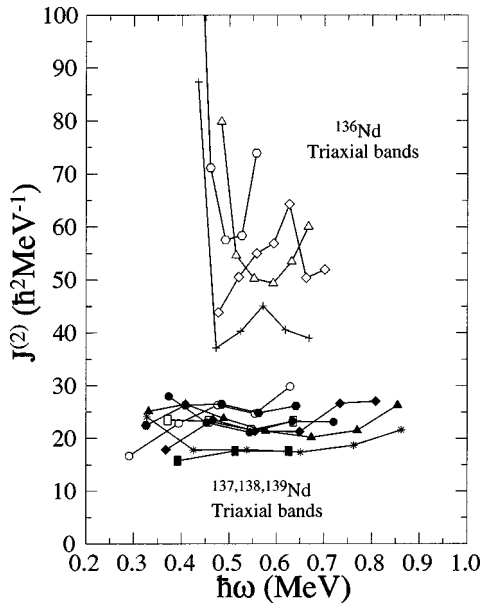
FIG. 3. Dynamical moments of inertia for the new triaxial bands observed in ^{138}Nd (band 1, filled hexagon; band 2, filled diamond; band 3, filled circle; band 4, filled rectangle) and ^{139}Nd (band 1, filled triangle; band 2, star). The moments of inertia of some triaxial bands of ^{136}Nd (band 1, open triangle; band 2, cross; band 4, open hexagon; band 6, open diamond) and ^{137}Nd (band 3, open circle; band 4, open rectangle) are also shown for comparison.

FIG. 4. Comparison between experimental and calculated configurations for ^{139}Nd. Solid and dashed lines are used for positive and negative parity configurations, respectively. Dotted lines are used for the experimental bands with unknown parity.

of the lowest state of band 4 is 25. The two bands observed in ^{139}Nd decay towards high-spin states which were not previously seen and are not discussed in detail here. Band 1 decays by means of a 388 keV $\Delta I = 1$ transition to the 47/2 level of a band with properties similar to bands 3 and 4 of ^{137}Nd [9], whereas band 2 decays by means of a cascade of two $E2$ transitions (1122 and 1033 keV) to a dipole band with properties similar to band 7 of ^{137}Nd. We assign spin 49/2 to the lowest state of band 1, even though a spin value larger by 2 cannot be excluded (due to possible unobserved transitions) and spin $\geq 49/2$ for the lowest state of band 2.

A general property of all the observed bands is a low and nearly constant dynamic moment of inertia, $J^{(2)}$ (see Fig. 3), with values which are around one third of the moment of inertia of a rigid rotor with a quadrupole deformation of $\varepsilon_2 = 0.25$. In addition, the $J^{(2)}$ values are less than approximately one half of the corresponding kinematic moments of inertia $J^{(1)}$ in the observed rotational frequency range, if the spin assignments discussed above are adopted. Moreover, the $J^{(1)}$ moments of inertia are smoothly decreasing functions of $\hbar\omega$. All these facts indicate the lack of pair alignments in the observed frequency range and suggest that both the proton and the neutron pairing are substantially quenched. The flat $J^{(2)}$ moments of inertia of the presently discussed bands have different behavior than that of the smooth unfavored terminating bands observed in the $A \sim 110$ mass region, where the $J^{(2)}$ values decrease with spin [14]. To gain insight into the structure of the observed bands, cranked Nilsson-Strutinsky (CNS) calculations based on the Nilsson potential have been performed using the same set of parameters as in Ref. [3]. The formalism of this approach is discussed in detail in Refs.
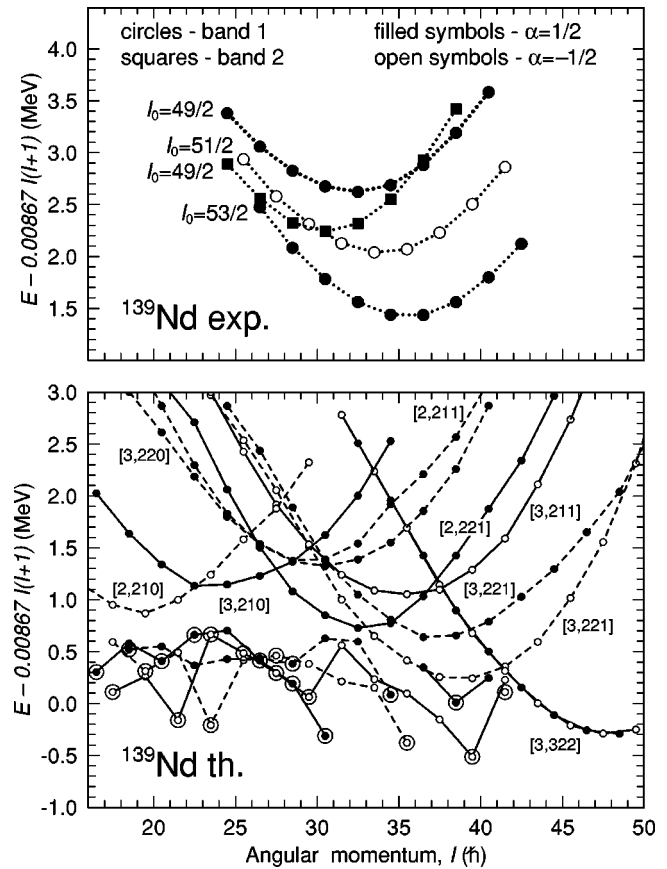
[3,14]. Note that pairing is neglected in these calculations. Comparisons between experimental and calculated ($E - E_{RLD}$) curves as a function of spin are given in Figs. 4 and 5, and the relation between curvatures in such plots and the $J^{(2)}$ moments of inertia is illustrated in Fig. 5. The discussion of possible configurations of the observed bands is based on the position of their minima in the experimental and calculated ($E - E_{RLD}$) plots. However, one should not compare the absolute energy scales. This is because the experimental level energies are given relative to the ground state energy, while the reference of the calculated levels is the liquid drop energy at $I = 0$. The calculated irregular yrast line is also shown, with the aligned (terminating) states encircled. The calculations suggest that we see nonyrast triaxial bands at spins higher than we can see the yrast band. This may be because the regular character of the triaxial bands is easier to identify than the irregular yrast band. When comparing theory and experiment in Figs. 4 and 5, the curves with the same type of symbols (open or closed) should be compared. The labeling of the calculated curves, $[p_1, n_1 n_2 n_3]$, is adopted to characterize the possible configurations in a compact form. The proton configurations are specified by the number of $h_{11/2}$ protons, p_1, while the neutron configurations are specified by the number of $h_{11/2}$ holes, n_1, relative to the $N = 82$ shell closure, followed by the number of neutron par-
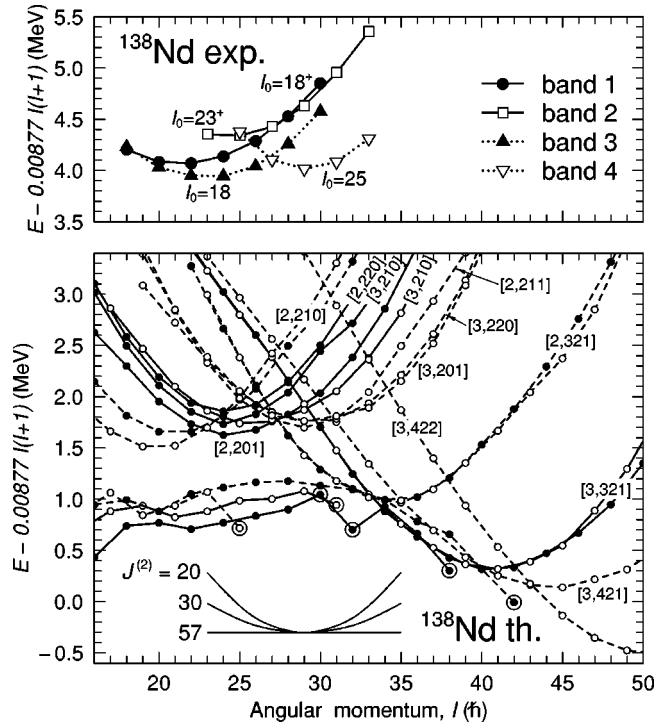
FIG. 5. Comparison between experimental and calculated configurations for ^{138}Nd. In the lower part of the figure, the curvature corresponding to some different values of $J^{(2)}$, expressed in $\hbar^2$ MeV^{-1}, is illustrated.

ticles in the $(h_{9/2}f_{7/2})$ and $i_{13/2}$ orbitals, n_2 and n_3.

Band 1 of ^{139}Nd is drawn in Fig. 4 (upper panel) with three possible spin assignments, with the lowest spin (49/2) being the most probable. If spin 49/2 is assigned to the lowest observed level, then configuration [2,221] is the most likely candidate with [3,220] and [2,211] as possible alternatives; if spin 51/2 or 53/2 is assigned, then the configuration [3,221] with signature $\alpha = -1/2$ (open symbols and solid line in the lower panel of Fig. 4) or the configuration [3,221] with $\alpha = +1/2$ (filled symbols and dashed line), respectively, are possible candidates. A similar analysis for band 2, which is drawn in the upper panel of Fig. 4 under the assumption of spin 49/2 for its lowest observed level, suggests [3,220] or [2,211] as possible configurations for this band (provided that they are not assigned to band 1). The comparison between the observed bands in ^{138}Nd and the calculated configurations is given in Fig. 5. The high density of calculated configurations with properties similar to the observed bands means that it is not very meaningful to make any detailed configuration assignments. However, it is easy to find calculated configurations which reproduce the general features of the observed bands, e.g., [2,201], [3,210] ($\alpha = 0$), and [2,220] for bands 1 and 3, [3,210] ($\alpha = 1$) for band 2 and [2,211], [3,220], or [3,201] for band 4.

The important feature common to all calculated configurations is that they have stable triaxial shapes with large positive γ values. The existence of a triaxial minimum in the spin range where the bands are observed is demonstrated by the potential energy surfaces (PES) used to extract the calculated energies in Figs. 4 and 5. The total PES for spin I^π
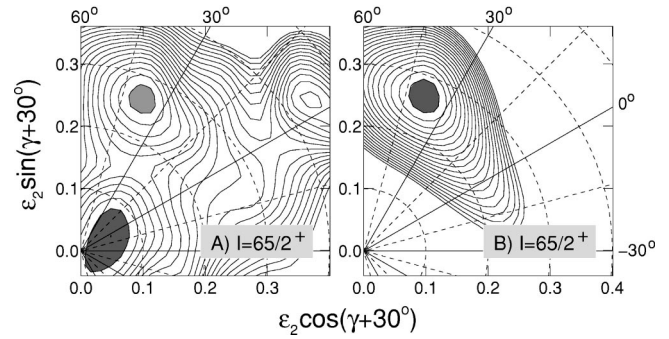

FIG. 6. Potential energy surfaces for ^{139}Nd calculated at spin $I = 65/2^+$ with only parity ($\pi = +$) and signature ($\alpha = +1/2$) fixed (left panel) and for the fixed configuration [2,221] (right panel). The contour line separation is 0.25 MeV.

$= 65/2^+$ in ^{139}Nd shown in the left panel of Fig. 6 has three minima: near-spherical, triaxial, and superdeformed. The right panel shows the PES for the fixed configuration [2,221]. The triaxial high-spin bands discussed here are characterized by having 1, 2 or, at most, 3 particles in each of several high-j shells, neutrons in $(h_{9/2}f_{7/2})$ and $i_{13/2}$, and protons in $h_{11/2}$. These particles are then relatively easy to align. Full alignment would lead to an oblate mass distribution around the rotation axis (noncollective rotation at $\gamma = +60°$). However, the other particles (holes) in open shells, the proton particles in $(g_{7/2}d_{5/2})$, and the neutron holes in $(d_{3/2}s_{1/2})$ and $h_{11/2}$, are much more difficult to align. They will counteract this coupling scheme, having a preference for collective rotation at $\gamma \approx 0°$ or $\gamma < 0°$. In the isotopes with N close to 82, there will be relatively few neutron holes (even with two or three particle-hole excitations across the $N = 82$ gap), so the polarization effects of the high-j particles towards $\gamma = 60°$ will dominate, leading to $\gamma = 30-40°$ for the full configurations in a large spin range. The comparatively stable triaxial deformation is typical for the calculated configurations of Figs. 3 and 4; for example, the [2,221] configuration shown in Fig. 6 evolves from $\varepsilon_2 = 0.27$, $\gamma = +32°$ at $I = 49/2$ to $\varepsilon_2 = 0.24$, $\gamma = +40°$ at spin $I = 81/2$. At some spin, non-negligible shape changes towards the noncollective axis at $\gamma = +60°$ are calculated to occur, but this does not happen until close to the terminating spin value ($I \approx 50$), where this band is calculated to lie far above yrast (see Fig. 4). The rigidity of the triaxial minimum is illustrated by the PES of the [2,221] configuration in Fig. 6, where at $I = 65/2$, the energy at the triaxial minimum is ~ 2 MeV below the lowest energy for oblate shape ($\gamma = +60°$) and ~ 3 MeV below the lowest energy for prolate shape ($\gamma = +0°$). The corresponding energy differences relative to oblate and prolate shape are ~ 3 MeV and ~ 2 MeV for $I = 49/2$, and ~ 1.2 MeV and ~ 2.6 MeV for $I = 81/2$, respectively.

For Nd isotopes with fewer neutrons, $N \approx 75$, the number of neutron holes is larger, and therefore the tendency towards collective rotation will be stronger. This explains why the high-spin bands in these nuclei are described by more collective configurations with $\gamma \approx 0°$ or $\gamma < 0°$.

The ^{137}Nd nucleus, with coexisting bands [9,15] similar

to both lighter and heavier Nd nuclei, marks the border between the lighter Nd nuclei where highly-deformed prolate $\nu i_{13/2}$ bands and triaxial bands with negative γ values dominate at high spins, and the ^{138,139}Nd nuclei where only triaxial bands with positive γ values are observed at high spins. The CNS calculations for this nucleus as presented in Ref. [3] show that the high-spin configurations with $3h_{11/2}$ protons and at least three $(h_{9/2}f_{7/2})$ and $i_{13/2}$ neutrons are comparatively collective but approach termination at high spin. However, for spin values $I<30$, configurations with only two $h_{11/2}$ protons are calculated yrast. In a similar way as for ^{138,139}Nd, these configurations are found to have an almost stable γ deformation of $30°-35°$ over a large spin range and, consequently, a small $J^{(2)}$ moment of inertia in agreement with the observed bands.

In summary, several rotational bands with small $J^{(2)}$ moments of inertia have been identified in ^{138,139}Nd over the spin range $I=20-40$. The regular character of these bands with no bandcrossings indicates that pairing correlations should be of minor importance. Indeed, the general features of the bands are reproduced in cranked Nilsson-Strutinsky calculations with no pairing. The corresponding configurations characterized by two to three neutrons excited across the $N=82$ gap are calculated to have a relatively stable triaxial deformation with $\gamma \approx +35°$ over the full spin range where the bands are observed. The small values of $J^{(2)}$, which are equivalently seen as a large curvature in E vs I plots, is interpreted as a specific fingerprint of triaxial deformation.

[1] R. Wyss *et al.*, Phys. Lett. B **215**, 211 (1988).
[2] C.M. Petrache *et al.*, Phys. Lett. B **335**, 307 (1994).
[3] A.V. Afanasjev and I. Ragnarsson, Nucl. Phys. **A608**, 176 (1996).
[4] C.M. Petrache *et al.*, Phys. Rev. C **57**, R10 (1998).
[5] C.M. Petrache *et al.*, Phys. Lett. B **373**, 275 (1996).
[6] K. Hauschild *et al.*, Phys. Rev. C **54**, 613 (1996).
[7] N.J. O'Brien *et al.*, Phys. Rev. C **59**, 1334 (1999).
[8] M. Piiparinen *et al.*, Nucl. Phys. **A605**, 191 (1996).
[9] C.M. Petrache *et al.*, Nucl. Phys. **A617**, 228 (1997).
[10] D. Ward *et al.*, Nucl. Phys. **A259**, 315 (1991).
[11] M. Müller-Veggian *et al.*, Nucl. Phys. **A344**, 89 (1980).
[12] G. de Angelis *et al.*, Phys. Rev. C **49**, 2990 (1994).
[13] J. Gizon *et al.*, J. Phys. G **4**, L171 (1978).
[14] A. V. Afanasjev, D. B. Fossan, G. J. Lane, and I. Ragnarsson, Phys. Rep. **322**, 1 (1999).
[15] C.M. Petrache *et al.*, Phys. Lett. B **219**, 145 (1996).